Journal of Alloys and Compounds 509 (2011) 744–747

Contents lists available at ScienceDirect

Journal of Alloys and Compounds

journal homepage: www.elsevier.com/locate/jallcom

One-pot facile synthesis and optical properties of porous $La_2O_2CO_3$ hollow microspheres

Helin Niu[a,*], Qiu Min[a], Zhiyin Tao[a], Jiming Song[a], Changjie Mao[a], Shengyi Zhang[a], Qianwang Chen[b]

[a] Department of Chemistry, Anhui University, Hefei 230039, PR China
[b] Hefei National Laboratory for Physical Sciences at Microscale, Department of Materials Science & Engineering, University of Science and Technology of China, Hefei 230026, PR China

ARTICLE INFO

Article history:
Received 11 June 2010
Received in revised form 4 September 2010
Accepted 8 September 2010
Available online 22 September 2010

Keywords:
Hollow structures
Lanthanum oxycarbonate
Hydrothermal
Photoluminescence

ABSTRACT

Lanthanum oxycarbonate ($La_2O_2CO_3$) hollow microspheres with novel porous architectures were successfully fabricated by a simple one-pot hydrothermal treatment of an aqueous solution containing glucose, $La(NO_3)_3{\cdot}6H_2O$, and subsequent calcination. The as-prepared $La_2O_2CO_3$ porous hollow spheres are composed of nanoparticles with a mean particle size of 15 nm. Carbon microspheres act as not only templates but also carbon sources for the formation of $La_2O_2CO_3$ hollow spheres. Interestingly, the as-prepared $La_2O_2CO_3$ hollow spheres show a green emission band under UV excitation, which may be used as fluorescent biological labels.

© 2010 Elsevier B.V. All rights reserved.

1. Introduction

Lanthanide compounds, as important member of rare earth (RE) materials, possess some phases, such as La_2O_3, $La(OH)_3$, $La_2O_2CO_3$. Much effort has been made for the studies of La_2O_3 which is very attractive for its applications in the fields of phosphors [1], catalysts [2] and catalyst supports [3,4]. The lanthanum oxycarbonate ($La_2O_2CO_3$), however, receives much less attention. $La_2O_2CO_3$ could be used as catalyst supports for hydrogen production [5]. Moreover, $La_2O_2CO_3$ is a novel rare earth luminescent material which exhibits bright green emission to the naked eyes under irradiation of the 320 nm UV lamp [6]. In fact, the impressive activity of La_2O_3 for methane coupling has been found earlier to be linked with $La_2O_2CO_3$ [7,8]. During the catalytic process, La_2O_3 was found to transform into hexagonal $La_2O_2CO_3$, which would suppress coking effectively, prevent the catalyst from sintering, and finally afford high dispersion of catalysts at elevated temperatures [2,9,10].

As is known to us all, the hollow spherical structures possess low density, large surface area, stability, surface permeability and well-aligned nanoporous structures, all of which make them attractive for scientific study. For instance, they might be used for nanoreactors [11], environmental applications [12], drug delivery [13,14], catalysts [15,16], batteries [17,18], supercapacitors [19], gas sensors [20], cancer SERS imaging [21], photoacoustic imaging [22], etc. Meanwhile, the hollow phosphors might radiate more light than its counterpart due to their interior hollow structure. Various synthetic strategies have been developed for the preparation of such hollow structures including template [23] and template-free methods [15], hydrothermal [24] and solvothermal approaches [25], ultrasound [13,16] and microwave assisted synthesis [26], Ion-exchange synthesis [20], saerosol route [27], chemical vapor deposition [28], Ostwald ripening [12], phase-inversion [29], excimer laser ablation [30] and ultra-high voltage hard anodization [31], and so on. However, to the best of our knowledge, there are few reports about hollow spherical $La_2O_2CO_3$ materials with photoluminescence (PL) properties.

Here, we report a simple one-pot method to prepare porous hollow microstructures $La_2O_2CO_3$ using hydrothermal treatment of glucose and $La(NO_3)_3{\cdot}6H_2O$, and subsequent calcination. The hydrothermal carbon microspheres act as not only templates but also carbon sources of the $La_2O_2CO_3$ hollow spheres. The advantage of this approach is to avoid a multistep process and is very attractive with high synthetic efficiency.

2. Experimental

2.1. Preparation methods

All reagents in analytic grade were used as received without further purification. In a typical experiment, 25 mmol glucose, 3 mmol $La(NO_3)_3{\cdot}6H_2O$ and 50 ml distilled water were added into a Teflon-lined stainless steel autoclave with 60 ml capacity. Then the autoclave was maintained at 180 °C for 4 h. The precipitate was filtered and washed with distilled water and ethanol, and finally dried at 80 °C for 6 h. The obtained products were calcined in air at 500 °C for 4 h to remove the carbon core.

* Corresponding author. Tel.: +86 551 5107342.
E-mail addresses: niuhelin@ahu.edu.cn, niuhelin@gmail.com (H. Niu).

0925-8388/$ – see front matter © 2010 Elsevier B.V. All rights reserved.
doi:10.1016/j.jallcom.2010.09.056

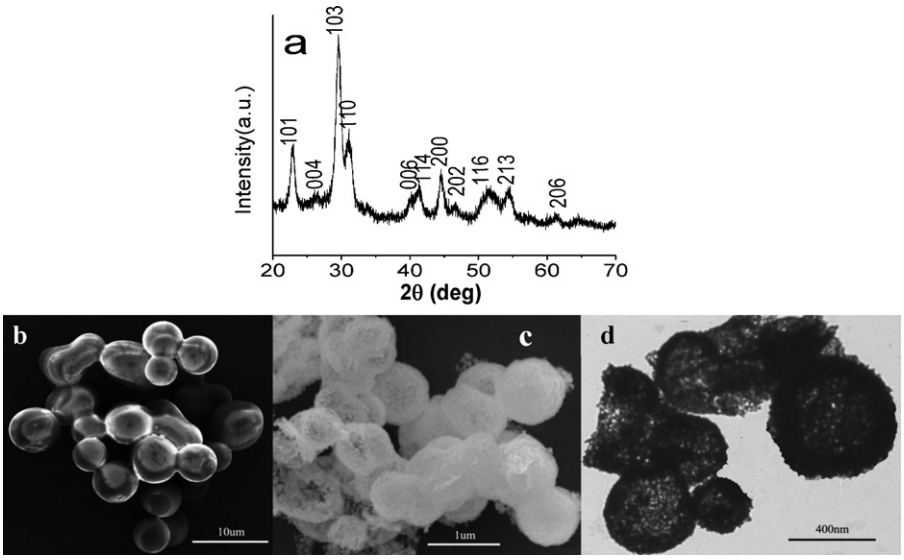

Fig. 1. XRD pattern (a) of the sample calcined at 500 °C for 4 h; SEM (b) image of the pre-calcined sample; SEM (c) and TEM (d) images of the sample calcined at 500 °C for 4 h.

2.2. Characterization

The as-prepared sample was characterized by X-ray diffraction (XRD, X'pert PRO SUPER, Cu Kα radiation, λ = 1.54056 Å), field emission scanning electron microscopy (FESEM, FEI Sirion 200), transmission electron microscopy (TEM, Hitachi H-800), ultraviolet–visible (UV–vis) diffuse reflectance spectroscopy (Hitachi U-4100) and photoluminescence spectroscopy (PL, Hitachi F-4500).

3. Results and discussion

3.1. Phase structures and morphologies

XRD is used to investigate the crystalline phases and crystallite size of the as-prepared samples before and after calcination. No crystalline peaks can be observed before calcination, indicating that the sample precalcination is amorphous, which confirms that after hydrothermal treatment, the metal ions are evenly dispersed in the hydrophilic shell of the carbon spheres as amorphous clusters. As shown in Fig. 1a, after calcination at 500 °C for 4 h, all the peaks of the products could be indexed to tetragonal $La_2O_2CO_3$ (JCPDS file no. 23-0320). No evidence of impurities can be found in the XRD pattern. Notably, the peaks are obviously broadened, a typical feature of nanostructured material, and the crystalline size is around 15 nm according to the Debye–Scherrer formula. The SEM image of the composite microspheres before calcination is shown in Fig. 1b, it is seen that the diameter of the microspheres is about 4–5 μm. The sample has poor monodispersity and a slight aggregation appears. Fig. 1c and d shows SEM and TEM images of $La_2O_2CO_3$ products, respectively. The products are relatively uniform and porous hollow spheres and possess diameters around 600–700 nm. The shell walls of the hollow spheres are composed of aggregated $La_2O_2CO_3$ nanoparticles of 15 nm in average size. A large number of pores with a size of about 30 nm can be seen on the spheres, suggesting that the sample is a kind of porous material.

3.2. Formation mechanism

The formation of La-based porous hollow spheres is assumed to involve two steps. The formation process is illustrated in Fig. 2.

First, considering the fact that the surface of carbonaceous polysaccharide microspheres is hydrophilic [24], which can bind La^{3+}, metal ions are supposed to be incorporated into their hydrophilic shell via the hydrothermal treatment of glucose/water/melt salt. Then, the sequential removal of carbon cores, densification, cross-linking, and phase transformation of La in the layer via calcination result in the formation of $La_2O_2CO_3$ hollow spheres. The reaction equations are expressed as follows:

$$La(C_6H_{12}O_6) + O_2 \rightarrow La_2O_2CO_3 + CO_2 + H_2O$$

When the calcination temperature was around 500 °C, carbon composite spheres with La^{3+} transformed to $La_2O_2CO_3$. It is obvious that the carbonaceous polysaccharide microspheres act as not

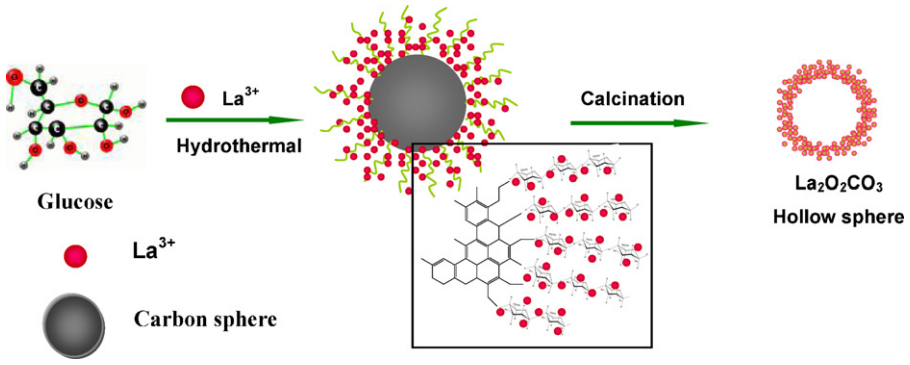

Fig. 2. Schematic illustration of the formation process for $La_2O_2CO_3$ hollow spheres.

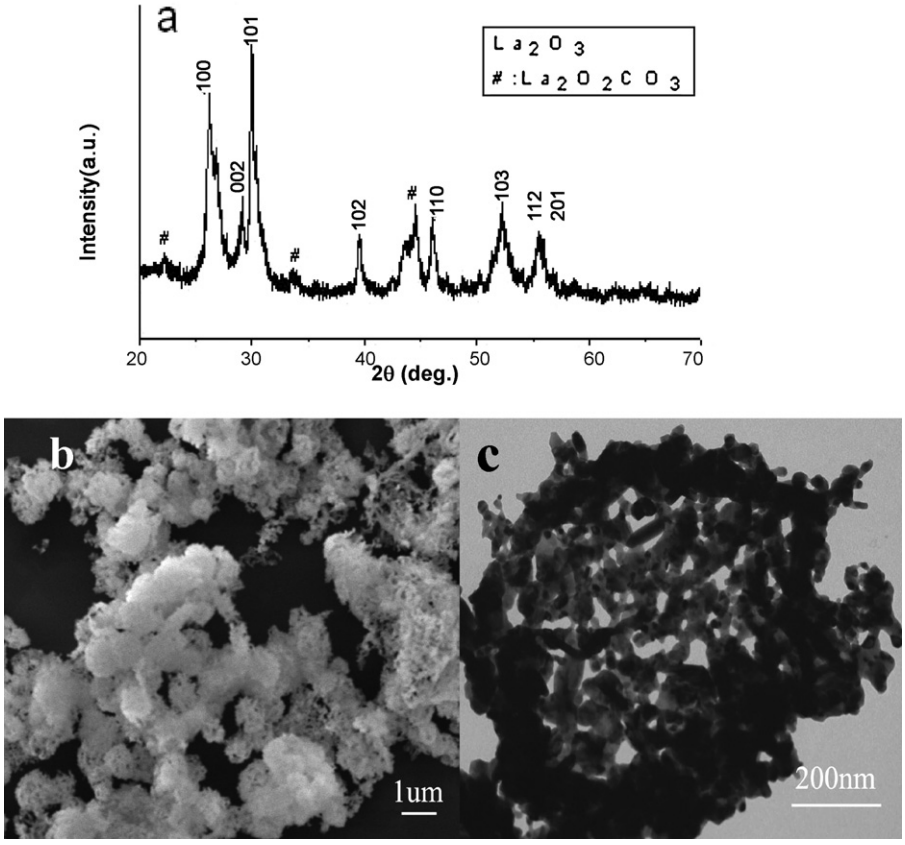

Fig. 3. XRD pattern (a), SEM (b) and TEM (c) images of the product calcined at 700 °C for 4 h.

only templates but also carbon sources for the formation of the $La_2O_2CO_3$ porous hollow spheres.

The temperature effect on the formation of $La_2O_2CO_3$ hollow spheres was studied. As above, the calcination for $La_2O_2CO_3$ hollow spheres was typically completed at 500 °C. If the calcination was performed below 400 °C, the $La_2O_2CO_3$ hollow spheres were not produced since the sufficient oxidization of the carbon composite spheres with La^{3+} could not take place at such low temperature [23]. However, the products calcined at 700 °C can be indexed to La_2O_3 (JCPDS card no. 74-2430) and hexagonal (II-) $La_2O_2CO_3$ (JCPDS card no. 25-0424) (Fig. 3a), among which La_2O_3 dominate, with an average crystalline size around 22 nm. As shown in Fig. 3b and c, compared to the samples calcined at 500 °C, the hollow spheres calcined at 700 °C show more broken spheres, and the shell is formed out of larger nanoparticles about 100 nm in size. This is because that tetragonal $La_2O_2CO_3$ was instable at above 500 °C, it would decompose into La_2O_3, i.e. $La_2O_2CO_3 = La_2O_3 + CO_2$ [32].

In addition, additive $Co(NO_3)_2{\cdot}6H_2O$ in the hydrothermal treatment process has a significant effect on crystallite phase of the final product. Fig. 4 shows the XRD patterns of the final products in the presence of $Co(NO_3)_2{\cdot}6H_2O$ after calcination at 500 °C for 4 h, the phase was hexagonal $La_2O_2CO_3$ (JCPDS card no. 25-0424) with poor crystallinity, compared with the tetragonal $La_2O_2CO_3$ in the absence of $Co(NO_3)_2{\cdot}6H_2O$. So, the addition of cobalt salt was believed to play the role of catalyst in the reaction or phase structures transformation. However, the true mechanism needs to be further investigated. Interestingly, there is no obvious Co-containing phase. This is probably because the smaller dosage of the cobalt content incorporated in the carbon shell than lanthanum, as well as the high dispersivity in the products.

3.3. UV–vis diffuse reflectance spectra and photoluminescence (PL)

Fig. 5a shows the UV–vis diffuse reflectance spectra of porous hollow $La_2O_2CO_3$ microspheres. A main absorption band at 252 nm for $La_2O_2CO_3$ is assigned to low-energy oxygen-to-metal charge transfer band [33]. The band at 380 nm can be attributed to the exciton band edge emission of $La_2O_2CO_3$ and the band at 460 nm is assigned to the green-wideband emission, which is the reasons for this result that the electron of oxygen vacancies combine with the hole in valence band. The luminescence spectra of the samples are shown in Fig. 5b. At an excitation wavelength of 252 nm, two luminescent bands can be found. One is a relative weaker UV band peaking at 368 nm, and the other is a stronger green emission

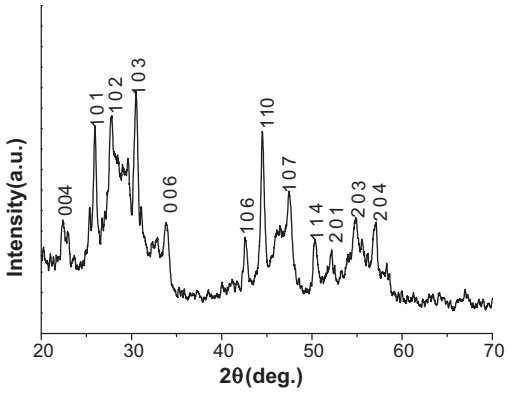

Fig. 4. XRD pattern of the product formed in the presence of $Co(NO_3)_2{\cdot}6H_2O$, followed by calcined at 500 °C for 4 h.

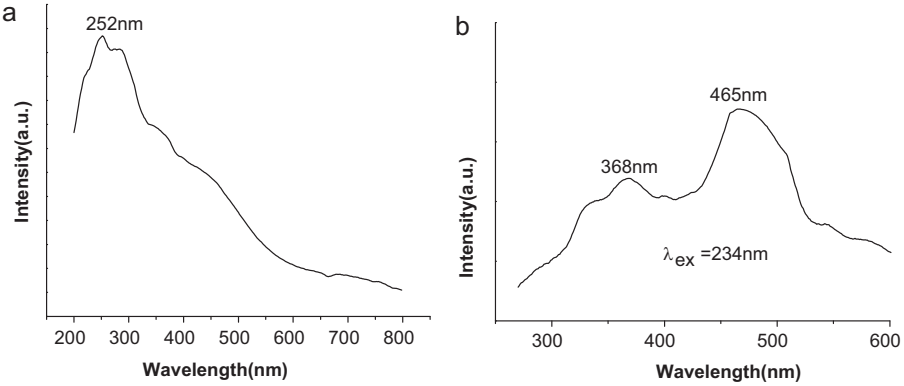

Fig. 5. UV–vis (a) diffuse reflectance spectrum and PL (b) emission spectrum of as-prepared hollow $La_2O_2CO_3$ microsphere.

band ranging from 430 to 530 nm centered at 465 nm, indicating the lower radiative photon energy compared with the absorption photon energy.

Based on the luminescence theory of rare-earth atoms, La^{III} shows a weak luminescence spectrum in the ultraviolet region as there is no f–f transition possible due to absence of 4f electrons in La^{3+}ions [33]. The UV emission shown in Fig. 5b may be due to the transition from the conduction band to the valence band, while the green emission may result from the radiative recombination of a photogenerated hole with an electron occupying an oxygen vacancy [10,34,35].

4. Conclusions

In summary, porous hollow $La_2O_2CO_3$ microspheres have been synthesized via a one-pot approach. The calcination temperature can influence the phase structures of the final products. The obtained lanthanum-based oxides materials show visible luminescence, implying their potential applications in biological labeling.

Acknowledgements

Support for this work from the National Science Foundation of China (Nos. 20875001, 20905001, 50901074), the Natural Science Foundation of Anhui Province (Nos. 090414200, KJ2010A014) and the 211 project of Anhui University are gratefully acknowledged.

References

[1] K. Koyabu, T. Masui, S. Tamura, N. Imanaka, J. Alloys Compd. 408–412 (2006) 867.
[2] H.Q. Chen, H. Yu, F. Peng, H.J. Wang, J. Yang, M.Q. Pan, J. Catal. 269 (2010) 281.
[3] J. Guzman, A. Corma, Chem. Commun. 6 (2005) 743.
[4] S. Irusta, L.M. Cornaglia, E.A. Lombardo, Mater. Chem. Phys. 86 (2004) 440.
[5] L.S. Jia, J.J. Li, W.P. Fang, J. Alloys Compd. 489 (2010) L13.
[6] X.Y. Fei, Z.W. Tao, J. Liu, X.B. Yu, J. Rare Earth 25 (2007) 342.
[7] D.C. Puxley, G.D. Squire, D.R. Bates, J. Appl. Crystallogr. 27 (1994) 585.
[8] R. Taylor, G. Schrader, Ind. Eng. Chem. Res. 30 (1991) 1016.
[9] A.N. Fatsikostas, D.I. Kondarides, X.E. Verykios, Catal. Today 75 (2002) 145.
[10] F. Frusteri, S. Freni, V. Chiodo, L. Spadaro, O.D. Blasi, G. Bonura, S. Cavallaro, Appl. Catal. A 270 (2004) 1.
[11] J.P. Deng, Y. Yu, S. Dun, W.T. Yang, J. Phys. Chem. B 114 (2010) 2593.
[12] Z.J. Yang, J.J. Wei, H. Yang, L.X. Liu, H. Liang, Y.Z. Yang, J. Eur. Chem. 21 (2010) 3354.
[13] M.L. Zhang, J. Chang, Ultrason. Sonochem. 17 (2010) 789.
[14] Y.F. Zhu, T. Ikoma, N. Hanagata, S. Kaskel, Small 6 (2010) 471.
[15] J.G. Yu, J. Zhang, Dalton Trans. 39 (2010) 5860.
[16] W. Liu, L.X. Cao, G. Su, H.S. Liu, X.F. Wang, L. Zhang, Ultrason. Sonochem. 17 (2010) 669.
[17] X.W. Guo, X. Lu, X.P. Fang, Y. Mao, Z.X. Wang, L.Q. Chen, X.X. Xu, H. Yang, Y.N. Liu, Electrochem. Commun. 12 (2010) 847.
[18] S.B. Yang, X.L. Feng, L.J. Zhi, Q.A. Cao, J. Maier, K. Mullen, Adv. Mater. 22 (2010) 838.
[19] P. Yu, X.O. Zhang, Y. Chen, Y.W. Ma, Mater. Lett. 64 (2010) 1480.
[20] J.G. Yu, J. Zhang, S.W. Liu, J. Phys. Chem. C 114 (2010) 13642.
[21] C.W. Huang, Y.W. Hao, J. Nyagilo, D.P. Dave, L.F. Xu, X.K. Sun, J. Nano Res. 10 (2010) 137.
[22] W. Lu, Q. Huang, K.B. Geng, X.X. Wen, M. Zhou, D. Guzatov, P. Brecht, R. Su, A. Oraevsky, L.V. Wang, C. Li, Biomaterials 31 (2010) 2617.
[23] X.M. Sun, J. Liu, Y.D. Li, J. Eur. Chem. 12 (2006) 2039.
[24] M.M. Titirici, M. Antonietti, A. Thomas, Chem. Mater. 18 (2006) 3808.
[25] L.F. Lai, G.M. Huang, X.F. Wang, J. Weng, Carbon 48 (2010) 3145.
[26] L. Zhang, X.F. Cao, Y.L. Ma, X.T. Chen, Z.L. Xue, Cryst. Eng. Commun. 12 (2010) 207.
[27] S. Gumen, B. Ebin, J. Alloys Compd. 492 (2010) 585.
[28] S.L. Wang, X. Jia, P. Jiang, H. Fang, W.H. Tang, J. Alloys Compd. 502 (2010) 118.
[29] Y.C. Cao, B. You, L.M. Wu, Langmuir 26 (2010) 6115.
[30] Z.J. Yan, R.Q. Bao, D.B. Chrisey, Nanotechnology 21 (2010) 145609.
[31] Y. Li, Z.Y. Ling, S.S. Chen, X. Hu, X.H. He, Chem. Commun. 46 (2010) 309.
[32] A.N. Shirsat, M. Ali, K.N.G. Kaimal, S.R. Bharadwaj, D. Das, Thermochim. Acta 399 (2003) 167.
[33] H. Yu, Q.Z. Zhai, J. Solid State Chem. 181 (2008) 2424.
[34] C.G. Hu, H. Liu, W.T. Dong, Y.Y. Zhang, G. Bao, C.S. Lao, Z.L. Wang, Adv. Mater. 19 (2007) 470.
[35] M.H. Huang, Y.Y. Wu, H. Feick, N. Tran, E. Weber, P.D. Yang, Adv. Mater. 13 (2001) 113.